

Supplementary Material

Microbial mat communities along an oxygen gradient in a perennially ice-covered Antarctic lake.

Anne D. Jungblut, Ian Hawes, Tyler J. Mackey, Megan Krusor, Peter T. Doran; Dawn Y. Sumner, Jonathan A. Eisen, Colin Hillman, Alexander K. Goroncy

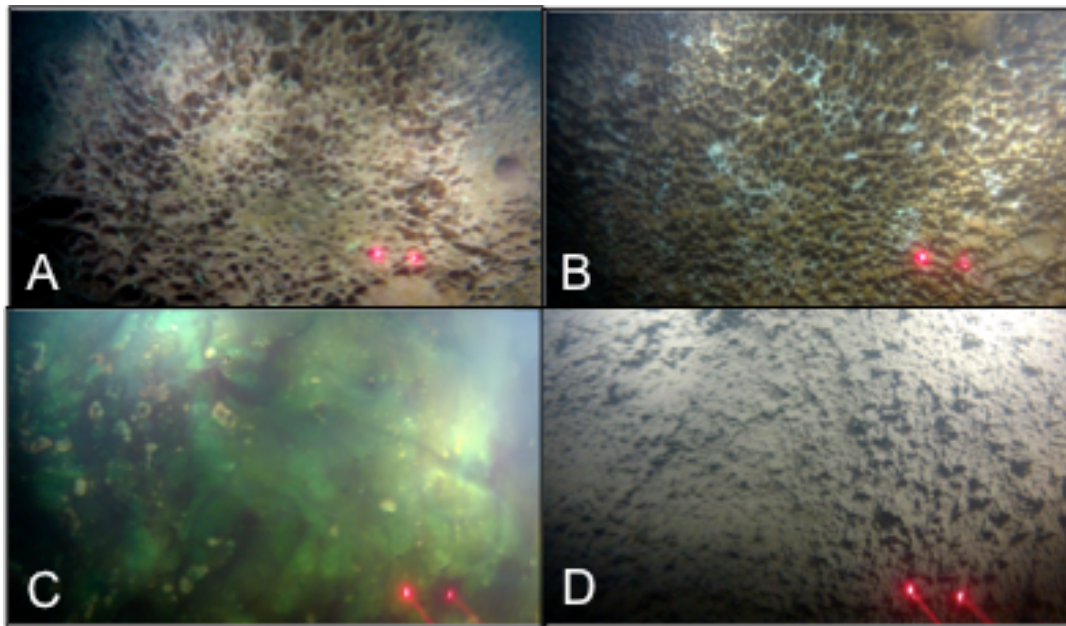
Supplementary Table S1.

Number of sequences and OTUs, Good's coverage and diversity indices for the nine microbial mat samples in Lake Fryxell, Antarctica.

| | Pinnacle mat | | | Ridge-Pit mat | | | Prostrate mat | | |
|-------------------------|--------------|--------|---------|---------------|--------|--------|---------------|--------|--------|
| | Top | Middle | Bottom | Top | Middle | Bottom | Top | Middle | Bottom |
| Number of OTUs | 4866 | 6210 | 5096 | 6492 | 7309 | 7050 | 4859 | 7174 | 6959 |
| Simpson diversity Index | 0.97 | 0.99 | 0.98 | 0.99 | 0.98 | 0.99 | 0.99 | 0.99 | 0.99 |
| Shannon Index | 7.33 | 8.26 | 7.84 | 8.12 | 7.96 | 8.31 | 5.16 | 8.12 | 8.14 |
| Chao Richness Estimator | 5581 | 7048 | 5963 | 7731 | 8518 | 8330 | 5966 | 8487 | 8225 |
| Ace Richness Estimator | 5474 | 6945 | 6117.79 | 7599 | 8472 | 8300 | 5904 | 8339 | 8157 |
| Good's Coverage (%) | 99.8 | 99.7 | 99.8 | 99.8 | 99.7 | 99.6 | 99.8 | 99.6 | 99.6 |

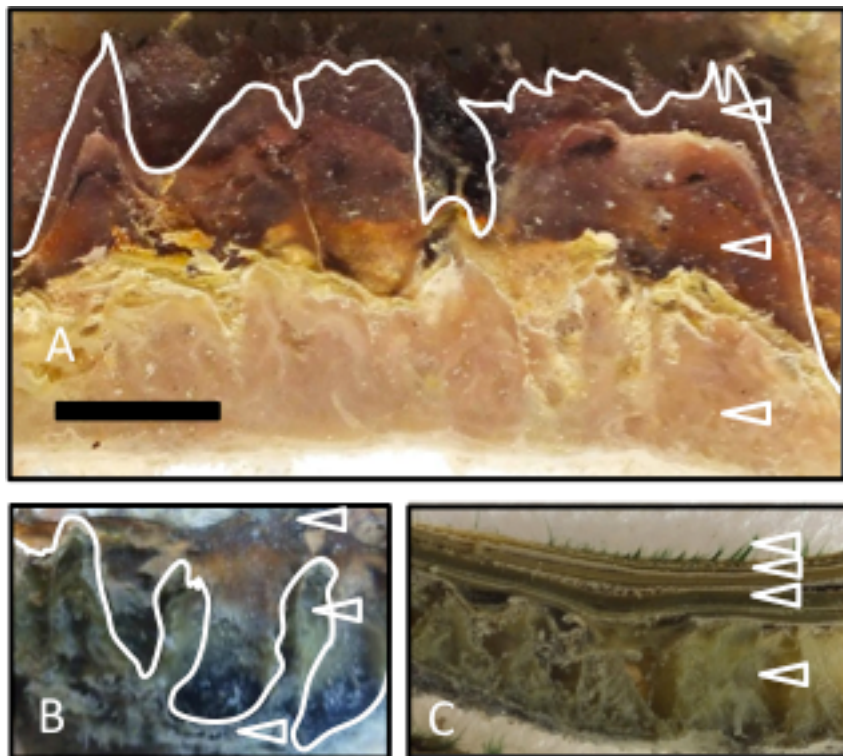
Supplementary Figure S1.

Macroscopic morphotypes of microbial mat such as cusped pinnacle (A), ridge-pit (B) and green prostrate mats (C) as well a (D) flocculent biomass zone seen along the oxygen transect in Lake Fryxell. In each image, two red dots are provided by parallel laser pointers separated by 3 cm.



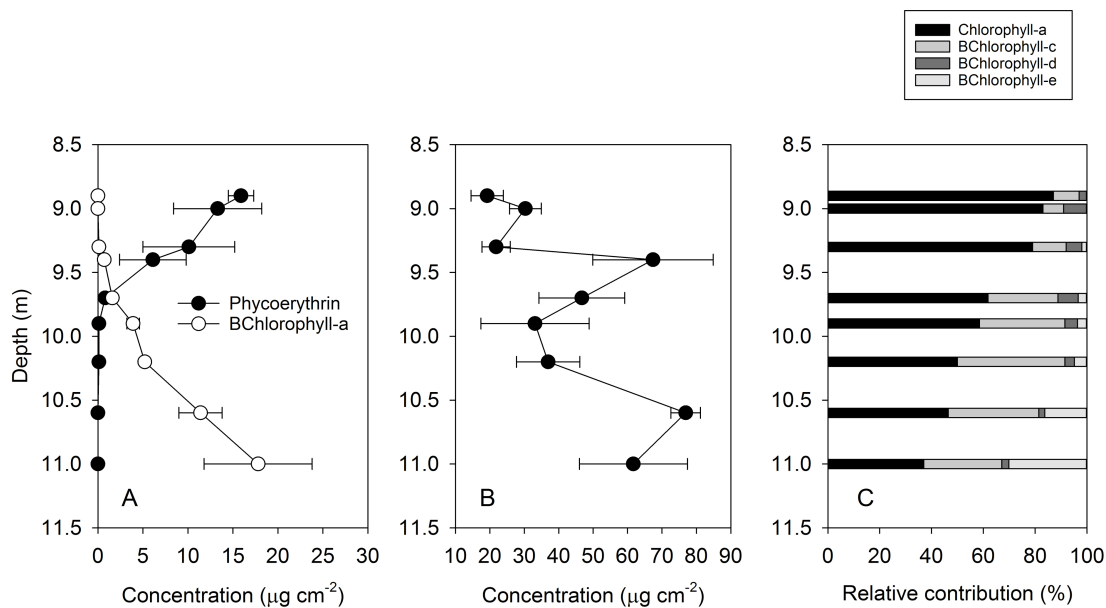
Supplementary Figure S2.

Vertical sections through pinnacle (A), ridge-pit (B) and green prostrate mats (C). The upper cut edge is traced with white outline for the pinnacle (A) and ridge-pit mats (B). Images are reproduced at a constant scale, indicated by the 10 mm bar at top. Black arrows indicate biomass zones that were selected for 16S rRNA gene analysis and isolation of the *Phormidium* morphotype.



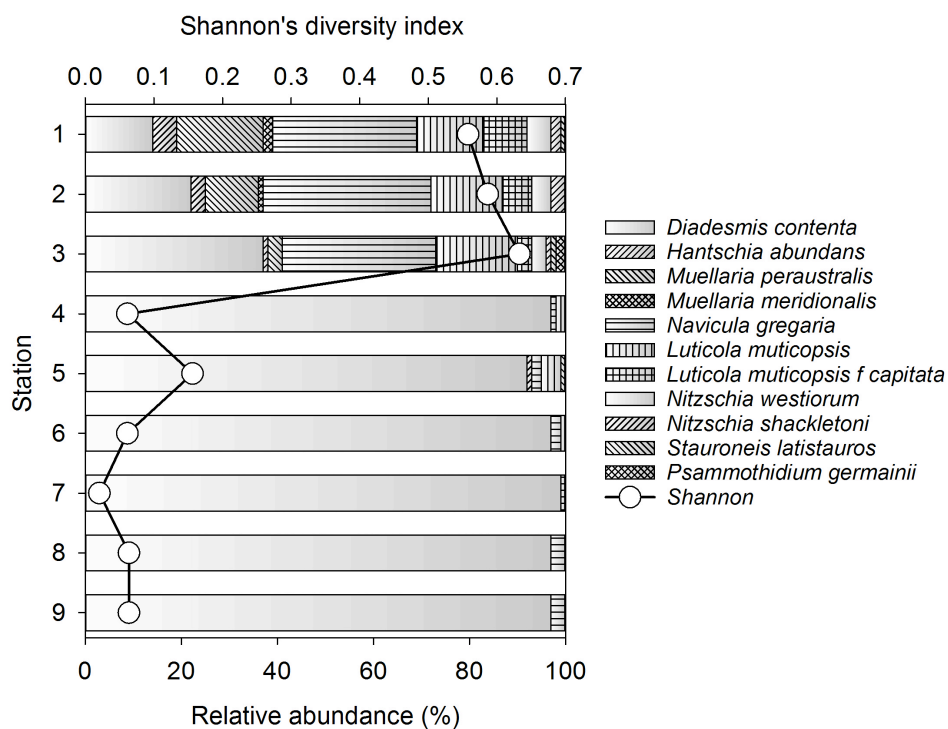
Supplementary Figure S3.

Concentrations of photosynthetic pigments estimated by spectrophotometry and HPLC of aqueous and acetone extracts at stations along the transect. A shows Bchl-a and Phycoerythrin, B shows “chlorophyll-a” as estimated by standard spectroscopic technique using absorption at 665 nm, and C shows the contribution of each recognizable pigment to absorption at 665 nm based on HPLC analysis.



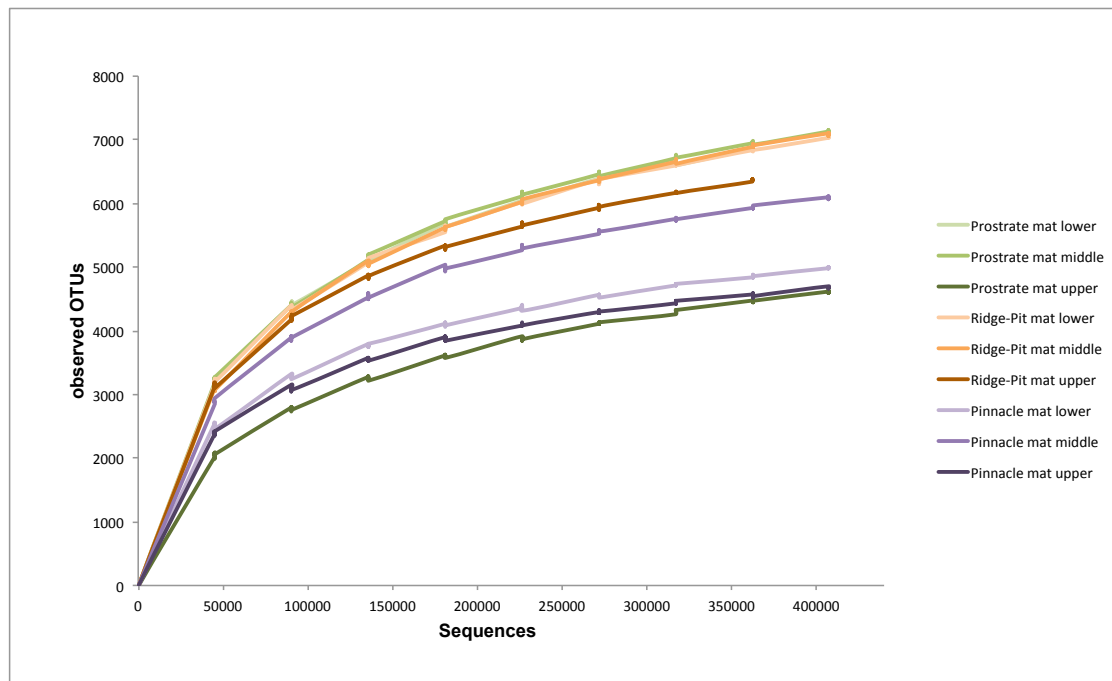
Supplementary Figure S4.

Relative abundance (%) of diatoms in samples and Shannon's diversity index (circles) from the nine transect sites in Lake Fryxell, Antarctica.



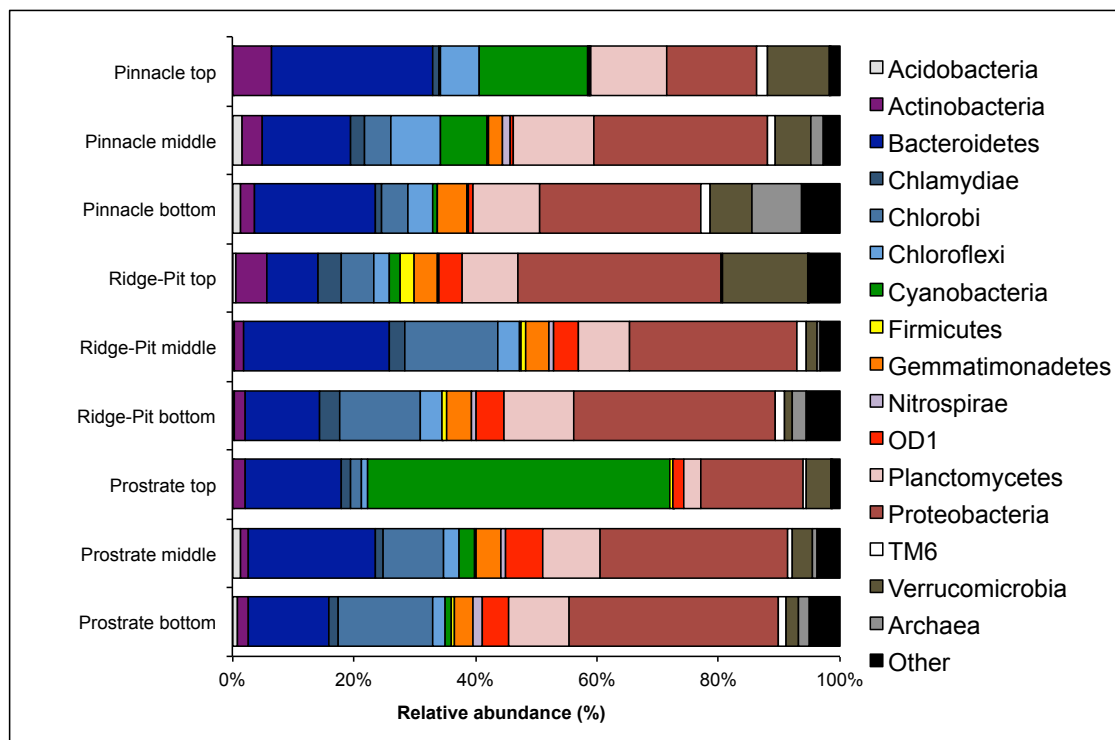
Supplementary Figure S5.

Rarefaction curves for in the upper, middle and lower mat layers in pinnacle, ridge-pit and prostrate mats.



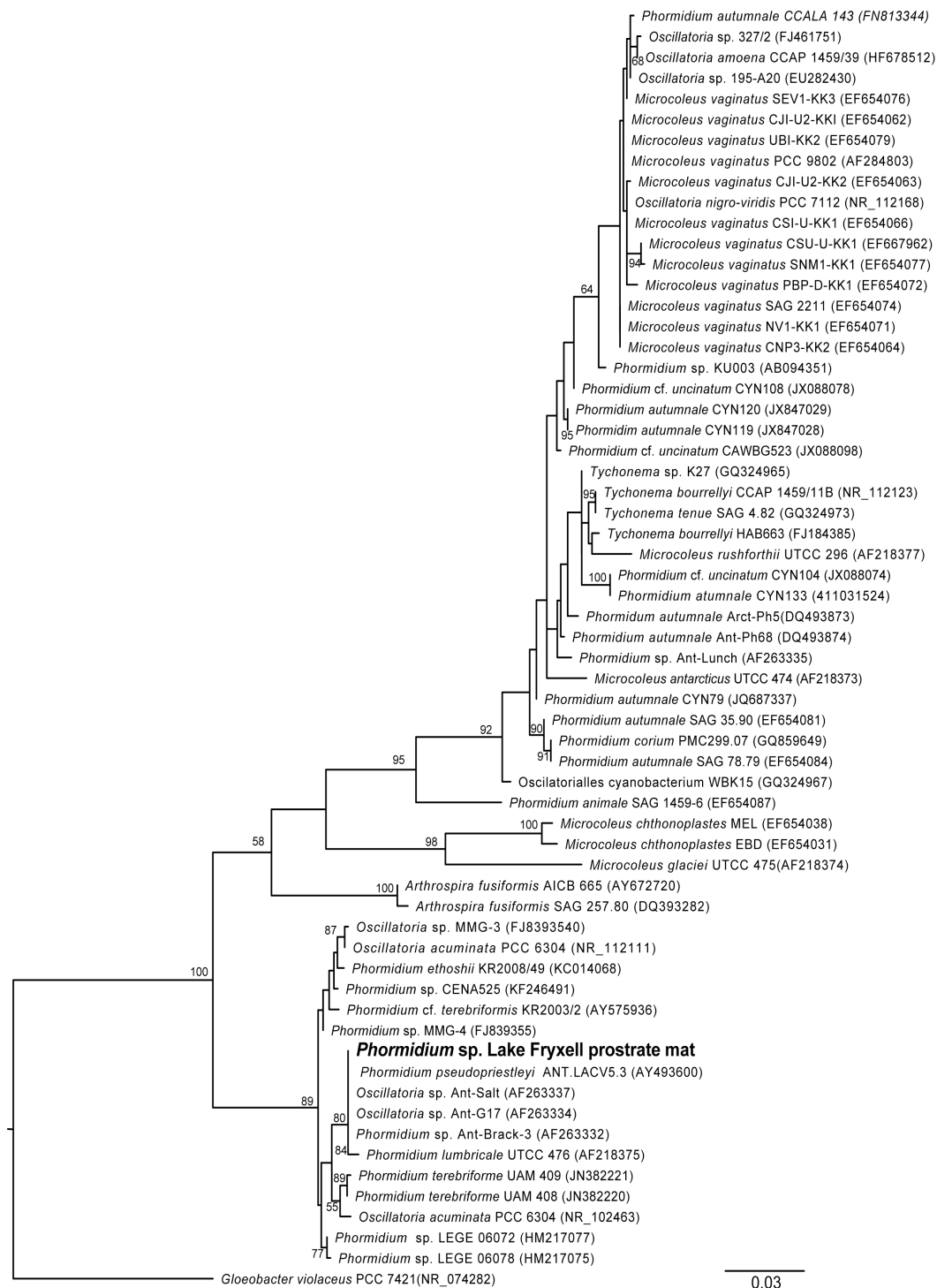
Supplementary Figure S6.

Relative abundance (%) of major bacterial phyla in the upper, middle and lower mat layers in pinnacle, ridge-pit and prostrate mats.



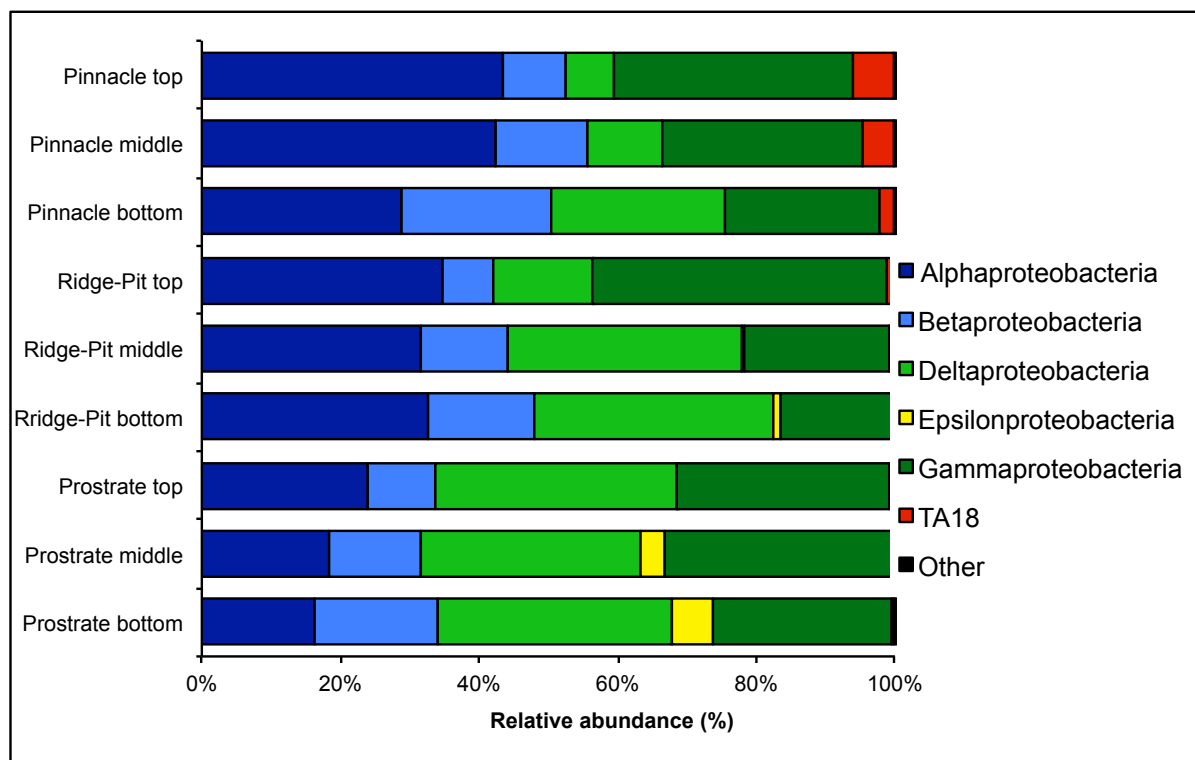
Supplementary Figure S7.

Phylogenetic analysis of *Phormidium* morphotype cyanobacterium isolated from the prostrate mat in Lake Fryxell, Antarctica.



Supplementary Figure S8.

Relative abundance (%) of major Proteobacteria classes in the top, middle and bottom mat layers in pinnacle, ridge-pit and prostrate mats.



Supplementary Figure S9.

Relative abundance (%) of Archaea classes in the top, middle and bottom mat layers in pinnacle, ridge-pit and prostrate mats.

